A STATISTICAL MODEL FOR DETERMINATION OF THE RADIATIVE TEMPERATURE AT 'BLACK-BODY' SURFACES

WILLIAM H. KEITH

A STATISTICAL MODEL FOR DETERMINATION OF THE RADIATIVE TEMPERATURE AT "BLACK-BODY" SURFACES, BASED UPON SPECIFIC WINDOW-RADIANCE VALUES MEASURED OVER A RANGE OF ZENITH ANGLES BY NIMBUS II RADIOMETER

by

William H. Keith
Lieutenant Commander, United States Navy
B.A., University of Wisconsin, 1953

Submitted in partial fulfillment
for the degree of

MASTER OF SCIENCE IN METEOROLOGY

from the

UNITED STATES NAVAL POSTGRADUATE SCHOOL
October 1966

ABSTRACT

Computed Channel 2 or window radiances for the Nimbus II optical-sensor system were kindly made available to the author by the Meteorological Satellite System of ESSA for each of the 106 model atmospheres considered by Wark et al. (1963)

Multiple regression equations relating the emitted black-body intensity from "black" interfaces to the independent variables (1) "observed" specific filtered radiance and (2) total optical path, were set up for each of seven zenith angles in the range $\theta = 0^{o}$ to 60^{o}, and for each of 62 randomly selected cases from the Wark sounding-catalog. Both variables gave high statistical significance, with the former accounting for the primary part of the variance of the dependent variable, but with variable (2) always contributing in such a way as to account for some of the atmospheric absorption along the sensing direction.

TABLE OF CONTENTS

Section		Page
1.	Introduction	7
2.	Data Sources	8
3.	Nature of the Data, and of the Model	9
4.	Data Processing	13
5.	Statistical Results and Inferences	14
6.	Estimation of Surface and Cloud Top Temperatures	20
7.	Angular-dependence Corrections & Conclusions	23
8.	Acknowledgements	26
9.	Bibliography	27
10.	Appendix I	28
11.	Appendix II	29

LIST OF ILLUSTRATIONS

Figure		Page
1.	First Estimate T_B as a Function of Filtered Window-Radiance	21

LIST OF TABLES

Table		Page
1.	Sample-set Employed in the Multiple Regression Analysis	15
2.	Multiple Linear Regression Equations Obtained from the BMD03R Program for Seven Zenith Angles	16
3.	Some Statistics Relating to the Multiple Linear Regression Equations for Seven Zenith Angles	18
4.	Corrections to First Estimates of $\hat{T}_B$ Based on Water Vapor Path for Zenith Angle $\theta = 0^o$	30
5.	Corrections to First Estimates of $\hat{T}_B$ Based on Water Vapor Path for Zenith Angle $\theta = 10^o$	31
6.	Corrections to First Estimates of $\hat{T}_B$ Based on Water Vapor Path for Zenith Angle $\theta = 20^o$	32
7.	Corrections to First Estimates of $\hat{T}_B$ Based on Water Vapor Path for Zenith Angle $\theta = 32.5^o$	33
8.	Corrections to First Estimates of $\hat{T}_B$ Based on Water Vapor Path for Zenith Angle $\theta = 45^o$	34
9.	Corrections to First Estimates of $\hat{T}_B$ Based on Water Vapor Path for Zenith Angle $\theta = 52.5^o$	35
10.	Corrections to First Estimates of T_B Based on Water Vapor Path for Zenith Angle $\theta = 60^o$	36

LIST OF SYMBOLS

Symbol	Meaning
F	flux of radiation
F_B	black-body flux of radiation
ΔF	flux loss
θ	zenith angle to sensor
$I(\theta)$	total specific intensity sensed at angle θ
$I_\emptyset(\theta)$	filtered specific intensity at angle θ
$I_\nu(\theta)$	monochromatic specific intensity at angle θ
$\Delta I(\theta)$	intensity depletion
T	temperature at interface
T_o	reference temperature (300K)
T_B	black-body temperature
$\widehat{T}_B$	best pooled-estimate of black-body temperature
$\Delta T_B(\theta)$	depletive correction to black body temperature
$dI_B/d\nu$	monochromatic black-body temperature
ν	wave frequency (in cm^{-1})
λ	wave length (in $\mu = 10^{-4}$ cm)
u	water vapor depth
u_*	reduced water vapor depth
$u_* \sec\theta$	reduced water vapor path
σ	Stefan-Boltzman constant
$A_i, B_i \cdots (i=1,2,3)$	best fit linear regression coefficients
MSL	Meteorological Satellite Laboratory of the Environmental Sciences Services Administration

1. Introduction

Wark et al. [7], and other authors have shown that both the surface air temperature under clear sky conditions, and the cloud-top temperature when the sky is covered by relatively dense clouds, as stratocumulus or altostratus, can be estimated using outgoing terrestrial radiation intensity observations obtained by Tiros II, III and IV channel 2 radiometers. Channel 2 radiometers are filtered to receive only infrared radiation in the "window" region of the spectrum, and in the Nimbus II this window region was 10-11μ . Usually the estimated temperature was several degrees too low under clear sky conditions.

By utilizing Nimbus II channel 2 radiometer computations of sensed outgoing terrestrial radiation intensity (as computed by the Meteorological Satellite Laboratory) for 62 atmospheric models -- all of the 47 cloud-undercast cases, and 15 randomly selected clear-sky cases, multiple linear regression equations are developed to solve for the angular dependence of total outgoing specific intensity $I(\theta)$ values. The multiple linear regression analysis uses the BMD03R program as adapted to the CDC 1604 computer.

In order to describe radiative temperatures at the earth's surface under clear sky conditions, and at the cloud-top for undercast conditions an estimate of the total specific intensity as viewed by Nimbus II must be made as a function of the emitted black body intensity and of an absorptivity dependent upon the effective optical path ($u_* SEC\,\theta$). Since, in general, window radiation is more readily available, it was decided to use specific filtered (window) radiation, rather than total specific intensity. The latter may then

be inferred as a function of interface temperature and optical path, as is done in Section 7.

Graphs/tables are then constructed which allow simple computation of the surface air temperature under clear skies, and cloud top temperatures, using total water vapor mass, zenith angle, and satellite radiometer measurements in Channel 2.

2. Data Sources

The data utilized consisted of the outgoing terrestrial radiation intensity computed by the Meteorological Satellite Laboratory from window region (Channel 2) data obtained from the Nimbus II satellite. 106 atmospheric models were developed by the Meteorological Satellite Laboratory in order to calculate the outgoing intensities [7], of which 62 selected cases are used in this paper. The 62 cases are composed of 47 cases undercast at various altitudes and 15 clear cases, which are identified in Appendix I. The models developed by the Meteorological Satellite Laboratory were taken from radiosonde data over all latitudes and seasons. All the soundings went to at least 25 mb, and the temperatures were extrapolated parallel to a standard atmosphere to the pressure of 0.1mb. Stratospheric humidity was extrapolated to conform in general to standard-atmosphere values. The sky condition, the temperature at selected levels and the temperature of the undercast level, as well as the total water vapor and ozone masses were also listed as part of the sounding catalog in [7].

In order to deduce total emergent flux and the angular dependence of these flux estimates, the specific filtered intensity in the 10-11μ

band for each of the 62 atmospheric models was used at each of the four given zenith angles ($\theta = 0^{o}$, 20^{o}, 45^{o} and 60^{o}). The intensities at three additional zenith angles ($\theta = 10^{o}$, 32.5^{o} and 52.5^{o}) were obtained by interpolation.

The radiation intensities of the 62 models were given in ERG/ (CM^2 SEC STRDN) and are converted to watts per meter^2 per strdn in this thesis.

3. Nature of the Data, and of the Model

The Nimbus II satellite uses both a High Resolution Infrared Radiometer (HRIR) scanning the 4.0 micron window, and a Medium Infrared Resolution Radiometer (MRIR) which scans the infrared spectrum in regions where the far infrared region of the solar spectrum gives only insignificant contributions. Only Channel 2 radiation of the MRIR segment is used, and the sensed radiation comes from an area of approximately 40 miles across in the horizontal (based upon a half-cone viewing angle of 2.9^{o}). The solid angle thus presented at the sensor is sufficiently small so that each measurement must be considered a specific intensity rather than flux.

The emergent flux is a more important quantity than that of outgoing specific intensity from the meteorological point of view, because the latter applies to a specific direction θ only, whereas the emergent flux gives total radiative heat loss from a column. In atmospheric radiation problems it is convenient to treat the ground and cloud surfaces as black bodies [1] . As shown in [3, pp. 81-82] the intensity and flux of radiation from a black body

are respectively

$$I_B = \frac{\sigma T^4}{\pi} \quad \text{AND} \quad F_B = \sigma T^4 \qquad (1)$$

in terms of the black-body surface temperature T_B. In (1), the constant σ of the Stefan-Boltzman law has the value

$$\sigma = 0.5664 \times 10^{-7} \text{ WATTS/M}^2$$

so that all values of F_B are in watts /m^2 and those of I_B are in watts/m^2/steradian.

The emergent filtered intensity, $I_{\oplus}(\theta)$, scans primarily the 10-11μ window region. The nature of the filter-transmissivity function in this band is an important consideration. The techniques by which the filter-functions are employed in conjunction with the sensor absorptivity is discussed in considerable detail by Wark et al [7, p. 3, and Supplement, p. 2.]. These same considerations have been applied to the measured values of $I_{\oplus}(\theta)$ for Nimbus II, and the computations provided by the Meteorological Satellite Laboratory are presumably available to other interested workers. The interesting facts are that (1) the thermister sensitivity is not unity in any of the wave band intervals, (2) that window filter function is not unity over the window, nor is it zero outside this spectral region. However, suffice it to say Wark's filtered radiance [7, Eq. 3] multiplied by the effective thermistor emissivity provides the "observed window radiation" of this study. Such data is of the form

$$I_{\oplus}(\theta) \doteq C \left(\frac{dI_B}{d\nu} \right)_{10}^{11} \qquad (2)$$

with C known as a quasi-constant with respect to $I_{\Phi}(\theta)$ over a wide angular range. Theoretically one could then enter a table of $I_{\Phi}(\theta)$ values, divide by C, and recover the appropriate temperature for $\left(\frac{dI_B}{d\nu}\right)$ from the Planckian monochromatic intensity function. However, even in the so called window region there are small atmospheric depletions due to both water vapor and ozone, which should be restored if accurate "black-surface" temperatures are to be estimated. Thus, in (3) below a depletive effect is added back to recover part of the initial beam intensity.

Hence the linear regression was set up with a heuristically physical basis, as follows:

$$\frac{\sigma T^4}{\pi} = A_0 + A_1 I_{\Phi}(\theta)\left[1 + A_2 u_* \left(\frac{T}{T_0}\right)^{1/2} \sec\theta\right] \qquad (3)$$

Here u_* has been multiplied by a single temperature-ratio correction factor of the Lorentz-type, since the individual computations of u_* did not include such factors in the layer-by-layer summations. The inclusion of this temperature-ratio term, along with the constant A_2, (to be determined) was aimed at inducing a more homogeneous stratification of the extinction treatment, since the cloud top cases investigated here varied considerably with respect to pressure level. Thus, (3) becomes

$$\frac{\sigma T^4}{\pi} = A_0 + A_1 I_{\Phi}(\theta) + A_2 A_1 \left(\frac{T}{T_0}\right)^{1/2} I_{\Phi}(\theta)\, u_* \sec\theta \qquad (4)$$

Moreover in view of the one-to-one (expected) relationship between $I_{\Phi}(\theta)$ and σT^4 remarked upon above, a linear statistical relationship of form

$$I_{\oplus}(\theta) = k_1(\sigma T^4) + k_2 \tag{5}$$

is proposed, with both k_1 and k_2 quite small. In fact, apart from sensor-noise, and second-order depletive effects, k_2 should be negligibly small and is treated thus here. (4) then assumes the form

$$\sigma T^4 = \pi A_0 + A_1(\pi I_{\oplus}(\theta) + \pi(A_2 A_1 k)\sigma T^4 \left(\frac{T}{T_0}\right)^{1/k} u_* \text{SEC}\,\theta \tag{6}$$

where A_0, A_1, A_2, and k would each have to be determined by standard best-fit methods. The grouping $\pi[I_{\oplus}(\theta)]$ is emphasized in order to show the conversion of intensity to flux units throughout (6). We therefore arrive at an alternative form of (6)

$$Y_1 = B_1 + B_2 X_2 + B_3 X_3 \tag{7}$$

where the independent variables are

$$X_2 = \pi I_{\oplus}(\theta)$$
$$X_3 = \sigma T^4 \left(\frac{T}{T_0}\right)^{1/2} u_* \text{SEC}\,\theta \tag{8a}$$

and the dependent variable is

$$Y_1 = \sigma T^4 \tag{8b}$$

The aim of the working equation, (7), is to determine how well the effective black-body temperature can be described statistically

by use of observed values of filtered radiance $I_{\Phi}(\Theta)$ and of a more complex variable X_3, which appears to depend upon the dependent variable, but actually its variance, $\sigma^2_{x_3} \approx CONST\left(\sigma^2_{u_* SEC\,\Theta}\right)$. However x_3 was formed as shown with values of u_* also known in advance for each of the 62 soundings used, in accordance with

$$u_* = \frac{1}{g}\int_{P=0.1\,MB}^{P_{SURFACE}} q\left(\frac{P}{1013.25}\right)\delta P \qquad (9)$$

The choice of the standard temperature $T_0 = 300^{\circ}K$ was used in connection with the full Lorentz-type broadening factor as set back into (3). This value was adopted based primarily upon experimental transmissivities of Palmer [5] who found that he could reproduce the theoretical absorption coefficients of Yamamoto as listed in [7], computed for $T = 260^{\circ}K$. This difference is well brought out by Wark et al. [7, eq. 5], which suggests that in order to retain u_* in the general format of (9), the exponent of (p/p_0) should be slightly less than unity. But then if strict conformity with Lorentz-type broadening is required, the standard temperature T_0 is raised to 300K.

4. Data Processing

As data samples for the testing of (7) at seven different angles in the range $\Theta = 0^{\circ}$ to 60°, the cloud-top and/or surface temperatures were used as input for $Y_1 = \sigma T^4$ for each of the 62 soundings chosen from M.S.L. Report Number 10 [7]. For each such sounding, values of $I_{\Phi}(\Theta)$ at angles $\Theta = 0^{\circ}, 20^{\circ}, 45^{\circ}, 60^{\circ}$, were also given for

Nimbus II. The $I_{\Phi}(\theta)$ sample was arbitrarily enlarged by linear interpolation to corresponding values at 10^{o}, 32.5^{o}, 52.5^{o}, giving seven angles for each sounding with seven corresponding values $I_{\Phi}(\theta)$. The variable

$$X_3 = (\sigma T^4)\left(\frac{T}{300}\right)^{1/2} u_* \sec\theta$$

was formed by transgeneration using a program available for this purpose at U.S. Naval Postgraduate School Computer Facility. There were 7 collections of punched data cards for each sample set (Y_1, X_2, X_3), each collection corresponding to a different zenith angle applied to the set of 62 soundings.

The multiple regression program BMD03R, as adapted to the CDC 1604, was utilized to solve for the value of the best fit coefficients for each of the seven zenith angles. The total input to the program consisted of 7x62 or 434 data cards. Table 1 shows a sample input for one zenith angle.

5. Statistical Results and Inferences

The multiple linear regression equations obtained from the program are shown in Table 2, in the form of (7) and (8). It can be readily seen by examining the formulas of Table 2, that the regression coefficient of the first independent variable considerably over-weights that variable when compared to the regression coefficient of the second variable, the depletion factor.

In order to examine the question of a significant specification of σT^4 by the independent variables X_2 and $X_3 = \sigma T^4 (\frac{T}{T_0})^{\frac{1}{2}} u_* \sec\theta$,

Table 1

Sample-set Employed in the
Multiple Regression Analysis *

θ	$X_2 = I_{\Phi}(\theta)$	X_3(watts/M^2)	Y_1(watts/M^2)
10	17.116	40.084	262.854
10	22.008	108.177	323.953
10	17.672	76.523	275.150
10	26.423	495.751	373.705
10	13.087	11.423	220.381
10	15.787	40.668	247.104
10	27.962	1071.279	406.182
10	16.987	50.299	262.854
10	24.897	399.156	363.327
10	21.474	129.534	319.265
10	25.129	181.637	363.327
10	8.635	1.694	158.511

*The above 12 samples represent 12 of 62 samples for the zenith angle $\theta = 10^{o}$.

Table 2

Multiple Linear Regression Equations Obtained from the BMD03R Program for Seven Zenith Angles

θ	Y_1	=	B_1	+	B_2 X_2	+	B_3 X_3
0^o	σT^4	=	58.270	+	$11.9226X_2$	+	$.01001X_3$
10^o	σT^4	=	58.869	+	$11.8840X_2$	+	$.01084X_3$
20^o	σT^4	=	52.412	+	$12.3788X_2$	+	$.00724X_3$
32.5^o	σT^4	=	62.265	+	$11.9233X_2$	+	$.00998X_3$
45^o	σT^4	=	56.224	+	$12.2479X_2$	+	$.00983X_3$
52.5^o	σT^4	=	57.978	+	$12.1866X_2$	+	$.01125X_3$
60^o	σT^4	=	63.657	+	$12.1443X_2$	+	$.01121X_3$

the F-statistics in Table 3 will be used as obtained from the output of the multiple linear regression program.

The BIMD03R program tests for significance of variables introduced into a multivariate linear regression equation. The most readily adaptable test, in the analysis of variance, is the so-called F-test where the

$$\text{F-statistic} = \frac{\text{Mean squares explained by predictor}}{\text{Mean squares unexplained}} \qquad (10)$$

In this experiment X_2 is the primary specifying variable, and for its test $F = F_{1,60}$ is defined as

$$F_{1,60} = \frac{\text{Sum of squares explained}}{\left[\frac{\text{Sum of squares unexplained}}{(N-2)}\right]}$$

The subscript numbering (1,60) denoted the number of degrees of freedom associated with numerator and denominator, respectively.

The addition of the depletion factor, symbolized by X_3, requires the definition of a new F-statistic specifically restricted to the testing of X_3, after the contribution of X_2 has been excluded. This statistic will be denoted F' and be defined as

$$F'_{1,59} = \frac{\text{Additional Sum of squares explained}}{\left[\frac{\text{Sum of squares unexplained}}{(N-3)}\right]} \qquad (11)$$

The critical value at the 99% confidence level of belief is 7.08 for both F and F', and these critical values are surpassed at the 99% confidence level for each variable added, with the exception of X_3 at $\theta = 20^0$ and 32.5^0. However the ratio

$$\frac{F_{1,60}(X_2)}{7.08} = O(10^2) \text{ to } O(10^3)$$

TABLE 3

Some Statistics Relating to the Multiple Linear Regression Equations for Seven Zenith Angles

θ	Variable	Mean	Reg.Coeff	Partial Corr Coeff	Mult Corr Coeff	Computed F & F' Values
0^o	X_2	19.690	11.92261	.99669		23927.718
	X_3	272.446	.01001	.55242		25.912
	Y_1	296.471			.9987	
10^o	X_2	19.681	11.88413	.99463		14765.000
	X_3	275.661	.01084	.49824		18.482
	Y_1	296.471			.9980	
20^o	X_2	19.620	12.37883	.96464		2088.534
	X_3	289.959	.00724	.14609		1.287
	Y_1	296.471			.9859	
32.5^o	X_2	19.436	11.92329	.96001		2972.724
	X_3	323.062	.00998	.24503		3.769
	Y_1	296.471			.9876	
45^o	X_2	19.248	12.24789	.99519		22457.562
	X_3	385.321	.00983	.61318		35.550
	Y_1	296.471			.9982	
52.5^o	X_2	19.131	12.18661	.98884		7231.164
	X_3	458.220	.01125	.56546		27.733
	Y_1	296.471			.9959	
60^o	X_2	18.720	12.14434	.94758		1427.700
	X_3	544.308	.01121	.36280		8.943
	Y_1	296.471			.9798	

and is so far beyond critical that the contribution of X_2 is highly significant, and certainly cannot be accounted for by a chance contribution in any of the seven cases. The contribution of X_3 as test by $\frac{F'_{1,59}(X_3)}{7.08} > 1$ in all cases except $\theta = 20^0$ and 32.5^0.

It should be noted that the coefficient of the depletion factor X_3 is positive in all cases; that is, it helps to account for a small but significant part of absorption from the originating flux σT^4, which part has been absorbed in the atmosphere. It has therefore been tentatively concluded that all 7 angular regression formulas afford significant information with respect to the atmospheric depletion, as well as to the primary variable $I_\Phi(\theta)$. Here, in effect some weight is being given to the sign test of the regression coefficient of X_3, even for $\theta = 20^0$ and 32.5^0, where the F' test falls short. The F-test failure in the case $\theta = 32.5$ is due to the inclusion of $\theta = 20^0$ data in the formation of the $\theta = 32.5$ sample.

An explanation for the lack of significance of the depletion factor for $\theta = 20^0$ could lie in the interplay of water vapor and ozone radiations, weak as both of these are likely to be.

The shortcoming of the statistical model must be recognized: only one absorbing element has been introduced, namely water vapor, which absorbs weakly in the "window" region [7, fig. 3] of the atmosphere. In addition, the small ozone content introduces a moderate absorbing band where the water vapor concentration is sparse (15 km and above). The emergent intensity formula for a

single-absorber atmosphere is given by

$$I_\nu(\theta) = I_{B\nu}(T_{TOP}) + \sum \tau_{\bar{\nu}}(u_4 \sec\theta) \frac{\partial I_{B\bar{\nu}}}{\partial T}(\Delta T) \qquad (12)$$

and, in a wave number interval where two absorbers give overlapping, the transmissivity $\tau_{\bar{\nu}}$ is generally taken as the product of the individual transmission functions for the gases taken separately.

First of all it appears that in the direct computation of top-transmitted radiance, there may be an angle where overlap-effects give larger discrepancies than at extremely close or extremely distant angular ranges. Secondly, the statistical attempt of synthesizing two absorbers by putting in just water vapor could not account for all of the variance attributable to depletion. Minor variations in the proportionality constant C of (2) undoubtedly do occur for any given setting of filtering wave band limits.

On the whole, however, a physically-based statistical model which has a multiple correlation coefficient ≥ 0.98 is quite adequate for specification of the dependent variable, and in the present case, of accounting for approximately one-third of the unexplained variance left over when $I_\Phi(\theta)$ alone is used in specification.

6. Estimation of Surface and Cloud Top Temperatures

Utilizing the multiple regression equations listed in Table 2, for the seven zenith angles, Fig. 1 and Appendix II have been developed to afford close approximations of the surface and/or cloud-top temperatures. The basic input data for use in these

FIG. 1

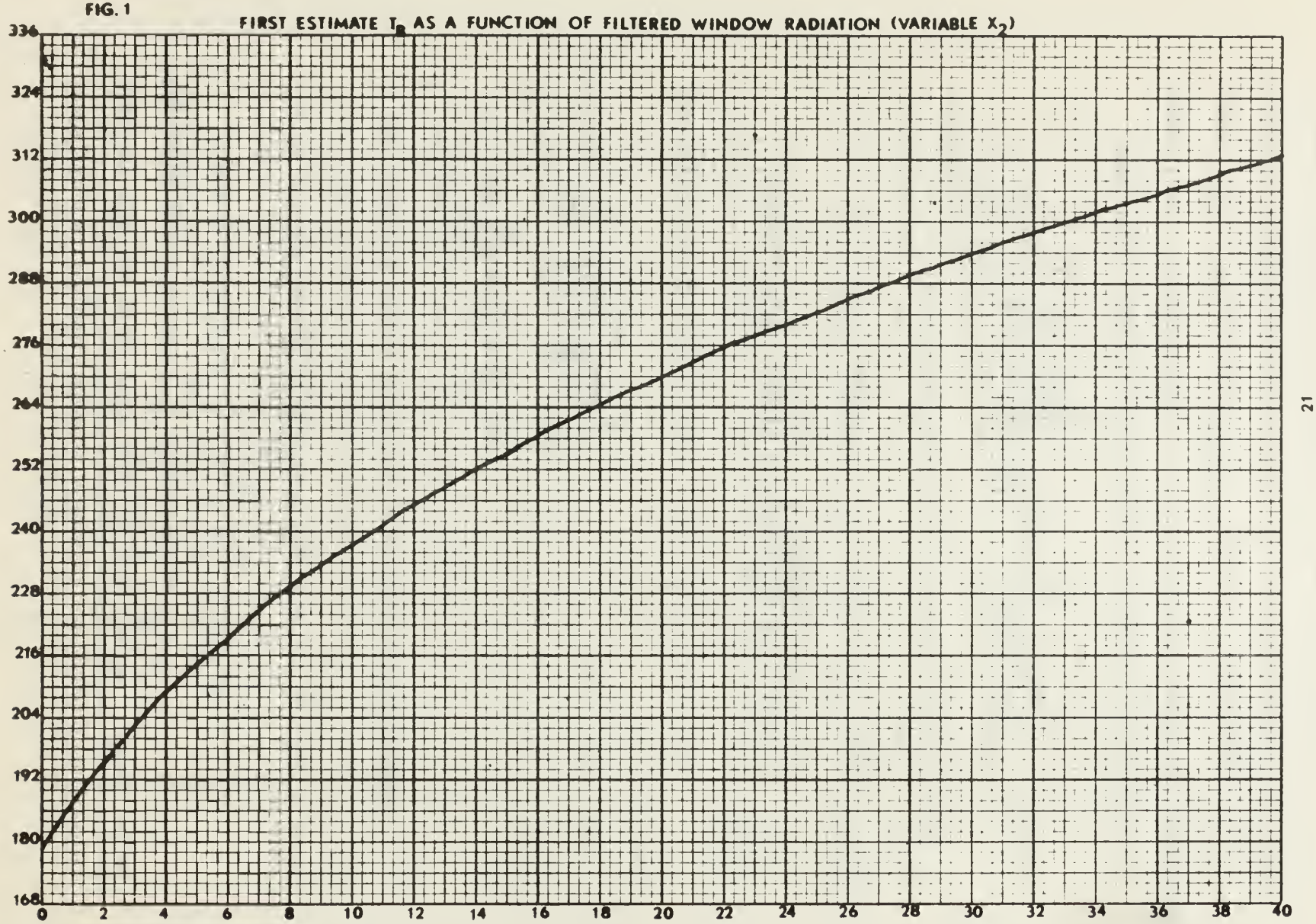
FIRST ESTIMATE T_B AS A FUNCTION OF FILTERED WINDOW RADIATION (VARIABLE X_2)
336
324
312
300
288
276
264
252
240
228
216
204
192
180
168
0
2
4
6
8
10
12
14
16
18
20
22
24
26
28
30
32
34
36
38
40

graphical aids are the Nimbus II Channel 2 radiation measurements, together with the water-vapor path in direction θ . These graphs are based upon (15) which is derived below.

Since by (7)

$$\sigma T^4 = B_1 + B_2 X_2 + B_3 X_3$$

we may define, a unique black-body flux using the mean values, $\bar{B}_1$ and $\bar{B}_2$:

$$\sigma \hat{T}_B^4 = \bar{B}_1 + \bar{B}_2 X_2$$

or

$$\hat{T}_B = \left[\frac{\bar{B}_1 + \bar{B}_2 X_2}{\sigma}\right]^{1/4} \tag{13}$$

Then making the approximation $\sigma T^4 = \sigma \hat{T}_B^4$ in X_3, we have

$$\sigma T^4 = \sigma \hat{T}_B^4 + B_3\left[\left(\sigma \hat{T}_B^4\right)\left(\frac{\overline{\sigma T_B}}{\overline{\sigma T_0^4}}\right)^{1/2} u_* \sec\theta\right] \tag{14}$$

By use of the binomial expansion carried out to the linear term only the water-vapor corrected radiative temperature is therefore given accurately by

$$T = \hat{T}_B + \left[\left(\frac{B_3}{4}\right)\left(\frac{\overline{\sigma \hat{T}_B^4}}{\overline{\sigma T_0^4}}\right)^{1/8} \sec\theta\right]\left[\hat{T}_B u_*\right] \tag{15}$$

From (15), a first estimate of the surface and/or cloud top temperature is obtained based upon the averaged form of the regression equation (7). This is justifiable insofar as (13) is concerned since the coefficients B_1 and B_2 vary from their means by only 5%, an insignificant deviation from the mean.

The bracketed factor in (15) may be written as a depletive correction to the interface temperature $\Delta T_B(\theta)$

$$\Delta T_B(\theta) = k(\theta)\,\hat{T}_B\,u_*$$

$$k(\theta) = \frac{B_3}{4}\left(\frac{\overline{\sigma \hat{T}_B^4}}{\overline{\sigma T_0^4}}\right)^{1/8} \sec\theta \qquad \theta = 0, \ldots, 60^\circ$$

Values for $\Delta T_B(\theta)$ are listed in Tables 4, 5.....10, for $\theta = 0^\circ$, 10°....., 60°, respectively. The input data for each table is $I(\theta)$ and the optical depth u_*.

Tests of the tables/graphs against known interface temperatures show very good results. The corrections ΔT_B are less than 2K, and usually less than 0.5K, but always additive in the sense of adding back depleted flux. In fact, the two steps just described, namely forming

$$\hat{T}_B + \Delta T_B$$

results in specification of the interface temperature T accurate to $\pm$ 0.2K. An alternative method for obtaining ΔT_B is discussed in Section 7.

7. Angular-Dependence Corrections and Conclusions

The major results derived have been the determination of a composite, pooled, first estimate of $\hat{T}_B$ from (13). Since $\hat{T}_B$ has been derived by averaging all of the nearly identical forms of the terms $B_1+B_2X_2$ of regression equation (7), $\hat{T}_B$ may be considered independent of the zenith angle.

The depletive correction $\Delta T_B(\theta)$ to the radiative temperature, arising from the presence of the water-vapor term was of the form

$$\Delta T_B(\theta) = k(\theta)\,\hat{T}_B\,u_*$$

in the regression equation (7, 15). Here k (θ) is a constant for each selection of θ , but differs from one zenith angle to the next.

To emphasize the nature of the angular dependency which now resides solely in the depletion term $\Delta T_B(\theta)$, consider the cases θ = 0° and 60°:

$$\theta = 0^\circ \qquad \Delta T_B(u_*, 0) = 2.366\,\hat{T}_B\,u_* \times 10^{-3}$$

$$\theta = 60^\circ \qquad \Delta T_B(u_*, \mathrm{SEC}\,60) = 5.298\,\hat{T}_B\,u_* \times 10^{-3}$$

This specialization is done not only because these results span completely the angular range employed, but also because both cases corresponded to significant F'-tests for variables X_3 in the analysis of variance (Section 4).

For intermediate values of θ, $\Delta T_B(\theta)$ may be estimated by the Taylor expansion formula applied in the form

$$\Delta T_B(\theta) \doteq \Delta T_B(\theta) + \left[\frac{\partial T_B}{\partial\,\mathrm{SEC}\,\theta}\right]\Delta(\mathrm{SEC}\,\theta) \qquad (16)$$

and when finite-differences are employed,

$$\Delta T_B(\theta) \doteq \Delta T_B(0) + \left[\frac{\Delta T_B(60) - \Delta T_B(0)}{1}\right](\mathrm{SEC}\,\theta - 1)$$

from which we finally obtain

$$\Delta T_B(\theta) = u_*\,\hat{T}_B\left[2.932\,\mathrm{SEC}\,\theta - 0.566\right] \times 10^{-3} \qquad (17)$$

(17) fits the results of Appendix II, Tables 4 - 10, within $\pm$ 0.2K and may be considered a good estimator of the best-fit depletive-correction for all angles θ in the range $0^\circ \leq \theta \leq 60^\circ$.

Further, the combination of (17) together with $\hat{T}_B$ of (13) led to the recovery of the known interface temperature to an accuracy of $\pm$ 0.2K.

As a measure of the effects of energy depletion, consider the intensity-depletion $\Delta I(\theta)$

$$\frac{\Delta I(\theta)}{I_B(\hat{T}+\Delta T)} \doteq \left\{\left[\sigma\left(\hat{T}_B+\Delta T_B\right)^4\right]-\sigma\hat{T}_B^4\right\}\Big/\sigma\hat{T}_B^4$$

or

$$\frac{\Delta I(\theta)}{I_B(\hat{T}_B)} = \frac{4\Delta T_B(\theta)}{\hat{T}_B} \qquad (18)$$

With regard to flux absorbed in the atmosphere, relative to the cloud-top estimate, $F_B(\hat{T}+\Delta T)$, one may integrate $\Delta I(\theta)$ hemispherically to obtain

$$\Delta F = 10^{-3} F_B(\hat{T}_B)\, u_* \int_0^{\pi/2} 4\left[2.932\,\mathrm{SEC}\,\theta - .566\right]\sin\theta\cos\theta\, d\theta$$

Upon integration, the last equation gives the flux-loss between interface and the channel 2 sensor

$$\Delta F \doteq F_B(\hat{T}_B)\, u_* \left[10.57 \times 10^{-3}\right] \qquad (19)$$

Here the last expression in the bracket shows the result of the integration. Limb-darkening has been neglected, since according to Wark et al [7] only about 25% of the possible flux lies outside of a 60^0 angle cone.

Even though the cloud temperature sensed by Channel 2 may be too low by 0.5^0 to 2.0^0, depending upon the zenith angle, the

"sensed" black-body intensity and flux values at cloud tops are too low by approximately 1 to 2% depending upon the actual value of $\Delta T_B(\theta)/\hat{T}_B$ of (17) and upon the value u_* in (19), respectively.

Refinements of this statistical model may be made to include a posteriori values of ozone or of dust-scattering, but such refinements are not likely to be as statistically significant on an operational basis where the optical masses of ozone and of dust are not known until long after the data readout is made.

Acknowledgments

The advice and encouragement of Professor Frank L. Martin of the United States Naval Postgraduate School are gratefully acknowledged.

BIBLIOGRAPHY

1. Craig, R.A. The Upper Atmosphere Meteorology and Physics. Academic Press, 1965.

2. Elsasser, W.M. and Culbertson, M.F. Atmospheric Radiation Tables. Meteorological Monographs. v. 4, No. 23, August, 1960.

3. Haltiner, G.J. and Martin, F.L. Dynamical and Physical Meteorology. McGraw-Hill, 1957.

4. Martin, F.L. and Palmer, W.C. Statistical Estimates of Computed Water-Vapor Radiative Flux from Clear Skies at an Oceanic Location. Journal of Applied Meteorology, v. 3, No. 6, December, 1964: 780-787.

5. Palmer, C.H. Experimental Transmission Functions for the Pure Rotation Bond of Water Vapor. Journal of the Optical Society of America, v. 50, 1960: 1232-1242.

6. Panofsky, H.A. and Brier, G.W. Some Applications of Statistics to Meteorology. University Park, Pennsylvania State University, 1963.

7. Wark, D.Q., Yamamoto, G. and Lienesch, J. Infrared Flux and Surface Temperature Determinations from Tiros Radiometer Measurements. U.S. Weather Bureau, Meteorological Satellite Laboratory, Meteorological Satellite Activities. Report no. 10, Aug. 1962 (Attached supplement dated April, 1963).

8. Wark, D.Q., Yamomoto, G. and Lienesch, J., Methods of Estimating Infrared Flux Surface Temperature from Meteorological Satellites. Journal of Atmospheric Science, v. 19, No. 6, September, 1962: 369-384

APPENDIX I

15 Clear Sky Atmospheric Models from [7]

Used in Multiple Linear Regression Program

Number	Location	Time
1	Havana, Cuba	1200 GMT, Sept. 29, 1958
2	Kenitra, Morocco	1200 GMT, Sept. 29, 1958
3	Oakland, California	1200 GMT, Sept. 29, 1958
4	Nantucket, Massachusetts	1200 GMT, Sept. 29, 1958
7	Ft. Smith, Arkansas	1200 GMT, Sept. 29, 1958
8	Thule, Greenland	1200 GMT, Sept. 29, 1958
10	Chaquaromos Bay, Trinidad	1200 GMT, April 1, 1958
12	Tucson, Arizona	1200 GMT, April 1, 1958
13	Washington, D.C.	1200 GMT, April 1, 1958
20	Clark Field, P.I.	1200 GMT, Jan. 1, 1958
23	Stephenville, Texas	1200 GMT, April 1, 1958
27	Glascow, Montana	1200 GMT, Jan. 1, 1958
31	Barter Island, Alaska	1200 GMT, Jan. 1, 1958
50	Chateauroux, France	1200 GMT, Jan. 25, 1958
51	Bitteurg, Germany	1200 GMT, Jan. 25, 1958

APPENDIX II

CORRECTIONS TO FIRST ESTIMATES OF $\hat{T}_B$ BASED ON WATER VAPOR PATH FOR ZENITH ANGLES $\theta = 10^o$, 32.5^o, 45^o, 52.5^o, and 60^o (Tables 4, 5, 6, 7, 8, 9 and 10)

TABLE 4

Corrections to First Estimates of $\hat{T}_B$ Based on Water Vapor Path for Zenith Angle

$\theta = 0^\circ$

$I(\theta)$ \ u_4	0.1	0.2	0.4	0.8	1.6	3.2
0	.0424	.0848	.1696	.3392	.6784	1.3568
2	.0462	.0924	.1848	.3696	.7392	1.4784
4	.0493	.0986	.1972	.3944	.7888	1.5776
6	.0517	.1034	.2068	.4126	.8272	1.6544
8	.0540	.1080	.2160	.4320	.8640	1.7280
10	.0561	.1122	.2244	.4488	.8976	1.7952
12	.0579	.1158	.2316	.4632	.9264	1.8528
14	.0595	.1190	.2380	.4760	.9520	1.9040
16	.0611	.1222	.2444	.4888	.9776	1.9552
18	.0620	.1240	.2480	.4960	.9920	1.9840
20	.0638	.1276	.2552	.5104	1.0208	2.0416
22	.0650	.1300	.2600	.5200	1.0400	2.0800
24	.0662	.1324	.2648	.5296	1.0592	2.1184
26	.0673	.1346	.2692	.5384	1.0768	2.1536
28	.0684	.1368	.2736	.5472	1.0944	2.1888
30	.0695	.1390	.2780	.5560	1.1120	2.2240
32	.0704	.1408	.2816	.5632	1.1264	2.2528
34	.0712	.1424	.2848	.5696	1.1392	2.3784
36	.0722	.1444	.2888	.5776	1.1552	2.3104
38	.0731	.1462	.2924	.5848	1.1696	2.3392
40	.0739	.1478	.2956	.5912	1.1824	2.3648

TABLE 5

Corrections to First Estimates of $\hat{T}_B$ Based on Water Vapor Path for Zenith Angle

$\theta = 10°$

$I(\theta)$ \ U_4	0.1	0.2	0.4	0.8	1.6	3.2
0	.0467	.0933	.1866	.3732	.7464	1.4928
2	.0508	.1016	.2032	.4064	.8128	1.6256
4	.0541	.1082	.2164	.4328	.8656	1.7312
6	.0569	.1138	.2276	.4552	.9104	1.8208
8	.0594	.1188	.2376	.4752	.9504	1.9008
10	.0615	.1230	.2460	.4920	.9840	1.9680
12	.0635	.1270	.2540	.5080	1.0160	2.0320
14	.0653	.1306	.2612	.5224	1.0448	2.0896
16	.0670	.1340	.2680	.5360	1.0720	2.1440
18	.0685	.1370	.2740	.5480	1.0960	2.1920
20	.0800	.1400	.2800	.5600	1.1200	2.2400
22	.0713	.1426	.2852	.5704	1.1408	2.2816
24	.0726	.1452	.2904	.5808	1.1616	2.3232
26	.0738	.1476	.2952	.5904	1.1808	2.3616
28	.0750	.1500	.3000	.6000	1.2000	2.4000
30	.0760	.1520	.3040	.6080	1.2160	2.4320
32	.0871	.1542	.3084	.6168	1.2336	2.4672
34	.0782	.1564	.3128	.6256	1.2512	2.5024
36	.0792	.1584	.3168	.6336	1.2672	2.5344
38	.0802	.1604	.3208	.6416	1.2832	2.5664
40	.0811	.1622	.3244	.6488	1.2976	2.5952

TABLE 6

Corrections to First Estimates of $\hat{T}_B$ Based on Water Vapor Path for Zenith Angle

$\theta = 20^\circ$

$I(\theta)$ \ U_A	0.1	0.2	0.4	0.8	1.6	3.2
0	.0314	.0628	.1256	.2512	.5024	1.0048
2	.0346	.0692	.1384	.2768	.5536	1.1072
4	.0371	.0742	.1484	.2968	.5936	1.1872
6	.0391	.0782	.1564	.3128	.6256	1.2512
8	.0410	.0820	.1640	.3280	.6560	1.3120
10	.0425	.0850	.1700	.3400	.6800	1.3600
12	.0440	.0880	.1760	.3520	.7040	1.4080
14	.0452	.0904	.1808	.3616	.7232	1.4464
16	.0464	.0928	.1856	.3712	.7424	1.4848
18	.0476	.0952	.1904	.3808	.7616	1.5232
20	.0486	.0972	.1944	.3888	.7776	1.5552
22	.0496	.0992	.1984	.3968	.7936	1.5872
24	.0505	.1010	.2020	.4040	.8080	1.4160
26	.0513	.1026	.2052	.4104	.8208	1.6416
28	.0521	.1042	.2084	.4168	.8336	1.6672
30	.0530	.1060	.2120	.4240	.8480	1.6960
32	.0536	.1072	.2144	.4288	.8576	1.7152
34	.0545	.1090	.2180	.4360	.8720	1.7440
36	.0551	.1102	.2204	.4408	.8826	1.7652
38	.0557	.1114	.2228	.4456	.8912	1.7824
40	.0563	.1126	.2252	.4504	.9008	1.8016

TABLE 7

Corrections to First Estimates of $\hat{T}_B$ Based on Water Vapor Path for Zenith Angle

$\theta = 32.5°$

$I(\theta)$ \ U_*	0.1	0.2	0.4	0.8	1.6	3.2
0	.0508	.1016	.2032	.4064	.8128	1.6256
2	.0550	.1100	.2200	.4400	.8800	1.7600
4	.0586	.1172	.2344	.4688	.9376	1.8752
6	.0615	.1230	.2460	.4920	.9840	1.9680
8	.0641	.1282	.2564	.5128	1.0256	2.0512
10	.0663	.1326	.2652	.5304	1.0608	2.1216
12	.0685	.1370	.2740	.5480	1.0960	2.1920
14	.0704	.1408	.2816	.5632	1.1264	2.2528
16	.0722	.1444	.2888	.5776	1.1552	2.3104
18	.0737	.1474	.2948	.5896	1.1792	2.3584
20	.0753	.1506	.3012	.6024	1.2048	2.4096
22	.0768	.1536	.3072	.6144	1.2288	2.4576
24	.0781	.1562	.3124	.6248	1.2496	2.4992
26	.0793	.1586	.3172	.6344	1.2688	2.5376
28	.0807	.1614	.3228	.6456	1.2912	2.5824
30	.0818	.1636	.3272	.6544	1.3088	2.6276
32	.0829	.1658	.3316	.6632	1.3264	2.6528
34	.0841	.1682	.3366	.6732	1.3464	2.6928
36	.0852	.1704	.3408	.6816	1.3632	2.7264
38	.0862	.1724	.3448	.6896	1.3792	2.7584
40	.0872	.1744	.3488	.6976	1.3952	2.7904

TABLE 8

Corrections to First Estimates of $\hat{T}_B$ Based on Water Vapor Path for Zenith Angle

$\theta = 45°$

$I(\theta)$ \ u_A	0.1	0.2	0.4	0.8	1.6	3.2
0	.0584	.1168	.2336	.4672	.9344	1.8688
2	.0639	.1278	.2556	.5112	1.0224	2.0448
4	.0683	.1366	.2732	.5464	1.0928	2.1856
6	.0720	.1440	.2880	.5760	1.1520	2.3040
8	.0752	.1504	.3008	.6016	1.2032	2.4064
10	.0780	.1560	.3220	.6240	1.2480	2.4960
12	.0806	.1612	.3224	.6448	1.2896	2.5792
14	.0828	.1656	.3312	.6624	1.3248	2.6496
16	.0849	.1698	.3396	.6792	1.3584	2.7168
18	.0869	.1738	.3476	.6952	1.3904	2.7808
20	.0888	.1776	.3552	.7104	1.4208	2.8416
22	.0906	.1812	.3624	.7248	1.4496	2.8992
24	.0923	.1846	.3692	.7384	1.4768	2.9536
26	.0938	.1876	.3752	.7504	1.5008	3.0016
28	.0953	.1906	.3812	.7624	1.5248	3.0496
30	.0967	.1934	.3868	.7736	1.5472	3.0944
32	.0982	.1964	.3928	.7856	1.5712	3.1424
34	.0994	.1988	.3976	.7952	1.5904	3.1808
36	.1007	.2014	.4028	.8056	1.6112	3.2224
38	.1019	.2038	.4076	.8152	1.6304	3.2608
40	.1031	.2062	.4124	.8248	1.6496	3.2992

TABLE 9

Corrections to First Estimates of $\hat{T}_B$ Based on Water Vapor Path for Zenith Angle

$\theta = 52.5^\circ$

$I(\theta)$ \ u_4	0.1	0.2	0.4	0.8	1.6	3.2
0	.0777	.1554	.3108	.6216	1.2432	2.4864
2	.0852	.1704	.3408	.6816	1.3632	2.7264
4	.0909	.1818	.3636	.7272	1.4544	2.9088
6	.0956	.1912	.3824	.7668	1.5336	3.0672
8	.0999	.1998	.3996	.7992	1.5884	3.1768
10	.1034	.2068	.4136	.8272	1.6544	3.3088
12	.1068	.2136	.4272	.8544	1.7088	3.4176
14	.1100	.2200	.4400	.8800	1.7600	3.5200
16	.1128	.2256	.4512	.9024	1.8048	3.6096
18	.1155	.2310	.4620	.9220	1.8440	3.6880
20	.1179	.2358	.4716	.9432	1.8864	3.7728
22	.1201	.2402	.4804	.9608	1.9216	3.8432
24	.1223	.2446	.4992	.9874	1.9568	3.9136
26	.2343	.2486	.4972	.9944	1.9888	3.9776
28	.1263	.2526	.5052	1.0104	2.0208	4.0416
30	.1281	.2562	.5124	1.0248	2.0496	4.0992
32	.1301	.2602	.5204	1.0408	2.0816	4.1632
34	.1317	.2634	.5268	1.0536	2.1071	4.2144
36	.1335	.2670	.5340	1.0680	2.1360	4.2720
38	.1350	.2700	.5400	1.0800	2.1600	4.3200
40	.1366	.2732	.5464	1.0928	2.1856	4.3712

TABLE 10

Corrections to First Estimates of $\hat{T}_B$ Based on Water Vapor Path for Zenith Angle

$\theta = 60^\circ$

$I(\theta)$ \ u_4	0.1	0.2	0.4	0.8	1.6	3.2
0	.0989	.1979	.3957	.7914	1.5828	3.1657
2	.1072	.2145	.4290	.8580	1.7159	3.4318
4	.1139	.2278	.4555	.9111	1.8222	3.6444
6	.1198	.2395	.4791	.9582	1.9164	3.8327
8	.1246	.2492	.4983	.9966	1.9932	3.9865
10	.1292	.2584	.5169	1.0338	2.0676	4.1351
12	.1332	.2662	.5327	1.0653	2.1306	4.2612
14	.1369	.2738	.5476	1.0951	2.1902	4.3805
16	.1404	.2808	.5616	1.1232	2.2464	4.4928
18	.1434	.2867	.5735	1.1470	2.2939	4.5878
20	.1463	.2927	.5854	1.1707	2.3414	4.6829
22	.1494	.2988	.5977	1.1953	2.3907	4.7814
24	.1518	.3037	.6074	1.2148	2.4296	4.9591
26	.1547	.3093	.6186	1.2372	2.4745	4.9490
28	.1568	.3136	.6273	1.2545	2.5091	5.0181
30	.1594	.3139	.6374	1.2748	2.5497	5.0993
32	.1616	.3231	.6463	1.2925	2.5851	5.1702
34	.1635	.3269	.6538	1.3077	2.6153	5.2307
36	.1657	.3315	.6629	1.3258	2.6516	5.3032
38	.1677	.3353	.6707	1.3414	2.6827	5.3654
40	.1684	.3368	.6737	1.3474	2.6948	5.3896

INITIAL DISTRIBUTION LIST

		No. Copies
1.	LCDR W.H. Keith Naval Weather Research Facility U.S. Naval Air Station, Bldg. R-48 Norfolk, Virginia 23511	3
2.	F.L. Martin Environmental Sciences U.S. Naval Postgraduate School Monterey, California	5
3.	Library U.S. Naval Postgraduate School Monterey, California 93940	2
4.	Department of Meteorology & Oceanography U.S. Naval Postgraduate School Monterey, California 93940	1
5.	Defense Documentation Center Cameron Station Alexandria, Virginia 22314	20
6.	Office of the U.S. Naval Weather Service U.S. Naval Station (Washington Navy Yard Annex) Washington, D.C. 20390	1
7.	Chief of Naval Operations OP-09B7 Washington, D.C. 20350	1
8.	Officer in Charge Naval Weather Research Facility U.S. Naval Air Station, Bldg. R-48 Norfolk, Virginia 23511	1
9.	Commanding Officer and Director Navy Electronics Laboratory Attn: Code 2230 San Diego, California 92152	1
10.	Officer in Charge Fleet Numerical Weather Facility U.S. Naval Postgraduate School Monterey, California 93940	2
11.	Director, Naval Research Laboratory Attn: Tech. Services Information Officer Washington, D.C. 20390	1

12. Geophysics Research Directorate
Air Force Cambridge Research Center
Cambridge, Massachusetts 1

13. Program Director for Meteorology
National Science Foundation
Washington, D.C. 1

14. U.S. Department of Commerce
Weather Bureau
Washington, D.C. 2

15. Office of Naval Research
Department of the Navy
Washington D.C. 20360 1

16. U.S. Naval Oceanographic Office
Attn: Division of Oceanography
Washington, D.C. 20390 1

17. Office of Naval Research
Department of the Navy
Attn: Geophysics Branch (Code 416)
Washington, D.C. 20360 1

18. Program Director Oceanography
National Science Foundation
Washington, D.C. 1

19. Director
National Oceanographic Data Center
Washington, D.C. 1

20. Chairman
Department of Meteorology & Oceanography
New York University
University Heights, Bronx
New York, New York 1

21. Director
Scripps Institution of Oceanography
University of California, San Diego
La Jolla, California 1

22. Department of Meteorology & Oceanography
Chairman
University of Hawaii
Honolulu, Hawaii 1

23. Department of Meteorology
University of California
Los Angeles, California 1

24. Department of the Geophysical Sciences
University of Chicago
Chicago, Illinois 1

25. Department of Atmospheric Science
Colorado State University
Fort Collins, Colorado 1

26. Department of Engineering Mechanics
University of Michigan
Ann Arbor, Michigan 1

27. School of Physics
University of Minnesota
Minneapolis, Minnesota 1

28. Department of Meteorology
University of Utah
Salt Lake City, Utah 1

30. National Center for Atmospheric Research
Boulder
Colorado 1

31. Department of Meteorology and Climatology
University of Washington
Seattle, Washington 98105 1

32. Department of Meteorology
University of Wisconsin
Madison, Wisconsin 1

33. Department of Meteorology
Florida State University
Tallahassee, Florida 1

34. Department of Meteorology
Massachusetts Institute of Technology
Cambridge, Massachusetts 02139 1

35. Department of Meteorology
Pennsylvania State University
University Park, Pennsylvania 1

36. University of Oklahoma
Research Institute
Norman, Oklahoma 1

37. Atmospheric Science Branch
Science Research Institute
Oregon State College
Corvallis, Oregon 1

38. The University of Texas
Electrical Engineering Research Laboratory
Engineering Science
Building 631A
University Station
Austin, Texas 78712 1

39. Department of Meteorology
Texas A & M University
College Station, Texas 77843 1

40. Lamont Geological Observatory
Columbia University
Palisades, New York 1

41. Division of Engineering and Applied Physics
Room 206, Pierce Hall
Harvard University
Cambridge, Massachusetts 1

42. Department of Mechanics
The Johns Hopkins University
Baltimore, Maryland 1

43. University of California
E.O. Lawrence Radiation Laboratory
Livermore, California 1

44. Department of Astrophysics and Atmospheric Physics
University of Colorado
Boulder, Colorado 1

45. Bureau of Meteorology
Department of the Interior
Victoria and Drummond Streets
Carlton, Victoria, Australia 1

46. International Antarctic Analysis Centre
468 Lonsdale Street
Melbourne, Victoria, Australia 1

47. Department of Meteorology
McGill University
Montreal, Canada 1

48. Central Analysis Office
Meteorological Branch
Regional Adm. Building
International Airport
Dorval, Quebec, Canada 1

49. Meteorological Office
315 Bloor Street West
Toronto 5, Ontario, Canada 1

50. Institut fur Theoretische Meteonologie
Freie Universitat Berlin
Berlin-Dahlem
Thiel-allee 49
Federal Republic of Germany 1

51. Meteorological Service
44, Upper O'Connell Street
Dublin 1, Ireland 1

52. Department of Meteorology
The Hebrew University
Jerusalem, Isreal 1

53. Geophysical Institute
Tokyo University
Bunkyo-ku
Tokyo, Japan 1

54. Department of Meteorology
Insituto de Geofisica
Universidad Nacional de Mexico
Mexico 20, D.F. , Mexico 1

55. New Zealand Meteorological Service
P.O. Box 722
Wellington, G.E. New Zealand 1

56. Institute of Geophysics
University of Bergen
Bergen, Norway 1

57. Department of Meteorology
Imperial College of Science
South Kensington
London S.W. 7, United Kingdom 1

58. Meteorological Office
London R.
Bracknell
Berkshire, United Kingdom 1

59. Commonwealth Scientific and Industrial Research
Organization
314 Albert Street
East Melbourne, C. 2, Victoria 1

60. Director
Pacific Oceanographic Group
Nanaimo, British Columbia
Canada 1

Security Classification

DOCUMENT CONTROL DATA - R&D

(Security classification of title, body of abstract and indexing annotation must be entered when the overall report is classified)

1. ORIGINATING ACTIVITY *(Corporate author)*
U. S. NAVAL POSTGRADUATE SCHOOL
Monterey, California 93940

2a. REPORT SECURITY CLASSIFICATION
UNCLASSIFIED

2b. GROUP

3. REPORT TITLE A STATISTICAL MODEL FOR DETERMINATION OF THE RADIATIVE TEMPERATURE AT "BLACK-BODY" SURFACES BASED UPON SPECIFIC WINDOW-RADIANCE VALUES MEASURED OVER A RANGE OF ZENITH ANGLES BY NIMBUS II RADIOMETER.

4. DESCRIPTIVE NOTES *(Type of report and inclusive dates)*
MASTER OF SCIENCE THESIS (METEOROLOGY)

5. AUTHOR(S) *(Last name, first name, initial)*
KEITH, William H.
Lieutenant Commander, U. S. Navy

6. REPORT DATE	7a. TOTAL NO. OF PAGES	7b. NO. OF REFS
	43	8

8a. CONTRACT OR GRANT NO.	9a. ORIGINATOR'S REPORT NUMBER(S)
b. PROJECT NO.	
c.	9b. OTHER REPORT NO(S) *(Any other numbers that may be assigned this report)*
d.	

10. AVAILABILITY/LIMITATION NOTICES
[redacted] obtain copies of this report from DDC
This document has been approved for public release and sale; its distribution is unlimited.

11. SUPPLEMENTARY NOTES	12. SPONSORING MILITARY ACTIVITY
	Chief of Naval Operations (OP-09B7) Department of the Navy Washington, D. C. 20360

13. ABSTRACT

Computed Channel 2 or window radiances for the Nimbus II optical-sensor system were kindly made available to the author by the Meteorological Satellite System of ESSA for each of the 106 model atmospheres considered by Wark et al (1963).

Multiple regression equations relating the emitted black-body intensity from "black" interfaces to the independent variables (1) "observed" specific filtered radiance and (2) total optical path, were set up for each of seven zenith angles in the range $\theta = 0^{o}$ to 60^{o}, and for each of 62 randomly selected cases from the Wark sounding-catalog. Both variables gave high statistical significance, with the former accounting for the primary part of the variance of the dependent variable, with variable (2) always contributing in such a way as to account for some of the atmospheric absorption along the sensing direction.

DD FORM 1 JAN 64 1473

Security Classification

14. KEY WORDS	LINK A		LINK B		LINK C	
	ROLE	WT	ROLE	WT	ROLE	WT
Satellite Radiation						
Window Radiation						
Nimbus II						
Radiative Temperature						

INSTRUCTIONS

1. ORIGINATING ACTIVITY: Enter the name and address of the contractor, subcontractor, grantee, Department of Defense activity or other organization *(corporate author)* issuing the report.

2*a*. REPORT SECURITY CLASSIFICATION: Enter the overall security classification of the report. Indicate whether "Restricted Data" is included. Marking is to be in accordance with appropriate security regulations.

2*b*. GROUP: Automatic downgrading is specified in DoD Directive 5200.10 and Armed Forces Industrial Manual. Enter the group number. Also, when applicable, show that optional markings have been used for Group 3 and Group 4 as authorized.

3. REPORT TITLE: Enter the complete report title in all capital letters. Titles in all cases should be unclassified. If a meaningful title cannot be selected without classification, show title classification in all capitals in parenthesis immediately following the title.

4. DESCRIPTIVE NOTES: If appropriate, enter the type of report, e.g., interim, progress, summary, annual, or final. Give the inclusive dates when a specific reporting period is covered.

5. AUTHOR(S): Enter the name(s) of author(s) as shown on or in the report. Enter last name, first name, middle initial. If military, show rank and branch of service. The name of the principal author is an absolute minimum requirement.

6. REPORT DATE: Enter the date of the report as day, month, year; or month, year. If more than one date appears on the report, use date of publication.

7*a*. TOTAL NUMBER OF PAGES: The total page count should follow normal pagination procedures, i.e., enter the number of pages containing information.

7*b*. NUMBER OF REFERENCES: Enter the total number of references cited in the report.

8*a*. CONTRACT OR GRANT NUMBER: If appropriate, enter the applicable number of the contract or grant under which the report was written.

8*b*, 8*c*, & 8*d*. PROJECT NUMBER: Enter the appropriate military department identification, such as project number, subproject number, system numbers, task number, etc.

9*a*. ORIGINATOR'S REPORT NUMBER(S): Enter the official report number by which the document will be identified and controlled by the originating activity. This number must be unique to this report.

9*b*. OTHER REPORT NUMBER(S): If the report has been assigned any other report numbers *(either by the originator or by the sponsor)*, also enter this number(s).

10. AVAILABILITY/LIMITATION NOTICES: Enter any limitations on further dissemination of the report, other than those imposed by security classification, using standard statements such as:

(1) "Qualified requesters may obtain copies of this report from DDC."

(2) "Foreign announcement and dissemination of this report by DDC is not authorized."

(3) "U. S. Government agencies may obtain copies of this report directly from DDC. Other qualified DDC users shall request through _____."

(4) "U. S. military agencies may obtain copies of this report directly from DDC. Other qualified users shall request through _____."

(5) "All distribution of this report is controlled. Qualified DDC users shall request through _____."

If the report has been furnished to the Office of Technical Services, Department of Commerce, for sale to the public, indicate this fact and enter the price, if known.

11. SUPPLEMENTARY NOTES: Use for additional explanatory notes.

12. SPONSORING MILITARY ACTIVITY: Enter the name of the departmental project office or laboratory sponsoring *(paying for)* the research and development. Include address.

13. ABSTRACT: Enter an abstract giving a brief and factual summary of the document indicative of the report, even though it may also appear elsewhere in the body of the technical report. If additional space is required, a continuation sheet shall be attached.

It is highly desirable that the abstract of classified reports be unclassified. Each paragraph of the abstract shall end with an indication of the military security classification of the information in the paragraph, represented as *(TS)*, *(S)*, *(C)*, *or (U)*.

There is no limitation on the length of the abstract. However, the suggested length is from 150 to 225 words.

14. KEY WORDS: Key words are technically meaningful terms or short phrases that characterize a report and may be used as index entries for cataloging the report. Key words must be selected so that no security classification is required. Identifiers, such as equipment model designation, trade name, military project code name, geographic location, may be used as key words but will be followed by an indication of technical context. The assignment of links, roles, and weights is optional.

DD FORM 1 JAN 64 1473 (BACK)